HOKKAIDO UNIVERSITY

Title	Estimation of S-Wave velocity structures in Avcilar-Istanbul from array microtremor measurements
Author(s)	Ozel, Oguz; SASATANI, Tsutomu; KUDO, Kazuyoshi; OKADA, Hiroshi; KANNO, Tatsuo; TSUNO, Seiji; YOSHIKAWA, Masataka; NOGUCHI, Shinako; MIYAHARA, Masakazu; GOTO, Hiroyuki
Citation	Journal of the Faculty of Science, Hokkaido University. Series 7, Geophysics, 12(2), 115-129
Issue Date	2004-03-22
Doc URL	http://hdl.handle.net/2115/8877
Type	bulletin (article)
File Information	12(2)_p115-129.pdf

Instructions for use

Estimation of S-Wave Velocity Structures in Avcilar-Istanbul from Array Microtremor Measurements

Oguz Ozel[1,2], Tsutomu Sasatani[1], Kazuyoshi Kudo[3],

Hiroshi Okada[1],

Tatsuo Kanno[4], Seiji Tsuno[3],

Masataka Yoshikawa[3], Shinako Noguchi[1],

Masakazu Miyahara[1]

and Hiroyuki Goto[5]

[1]*Division of Earth and Planetary Sciences, Graduate School of Science Hokkaido University, Sapporo 060-0810, Japan*
[2]*Kandilli Observatory and Earthquake Research Institute Bogazici University, Istanbul 81060, Turkey*
[3]*Earthquake Research Institute, University of Tokyo, Tokyo 113-0032, Japan*
[4]*Graduate School of Engineering, Hiroshima University, Hiroshima 739-8257, Japan*
[5]*Graduate School of Engineering, Kyoto University, Kyoto 606-8501, Japan*

Abstract

In September, 2003, we conducted array measurements of microtremors at two sites (AVC and DHM) in Avcilar, the west part of Istanbul, Turkey, to estimate the S-wave velocity structures; this is a continuation of the same type observations carried out just after the 17 August 1999 Izmit earthquake. Heavy damage occurred around the AVC site due to the Izmit earthquake and a permanent strong-motion station is deployed at DHM. We used the SPAC method in estimation of phase velocities of Rayleigh waves within microtremors, and the genetic algorithm in estimation of the S-wave velocity structures from the phase velocities. Then the empirical amplification functions derived from aftershock records were compared with the theoretical ones calculated based on the structures. We obtained reasonably a good agreement between them, except one site of the tripartite array stations in AVC. The S-wave velocity structures estimated in this study provide basic data for prediction of strong-ground motion in Istanbul.

1. Introduction

It is clear from the recent devastating earthquakes in Turkey that Istanbul is under a threat of unruptured segments of North Anatolian Fault zone. If an earthquake of similar magnitude as the 17 August 1999 earthquake (Mw 7.4) occurs in this region, it will result in an immeasurable impact on Istanbul City. From this point of view, it is essential to predict strong ground motion from a probable earthquake, which threatens Istanbul City. On the other hand, the theoretical simulation or prediction of strong-ground motions strongly requires getting subsurface S-wave velocity structures, especially for sedimentary layers overlying the bedrock. For the requirement, we think of applying conventional seismic method, i.e. reflection or refraction method to the area of interest. However, these methods are practically not easy to implement in an urban area. As a feasible alternative to the conventional seismic methods, an array observation of microtremors, i.e. microtremor survey method (MSM) (Okada, 2003 ; Aki, 1957) is available, which is a very promising and an easy method to apply especially to an urbanized area like Istanbul. The basic scheme of MSM consists of two steps. The first step is to extract the Rayleigh wave from microtremors in the form of dispersion ; that is, phase velocities of the Rayleigh wave are obtained as a function of frequency. The second step is to invert the phase velocities to subsurface structures, which are practically given by depth distribution of S-wave velocity.

In September and December 1999, soon after the 17 August 1999 Izmit earthquake, Kudo et al. (2002) performed array microtremor measurements beneath the permanent strong motion sites recording the mainshock, and also in the areas where heavy damage took place, in order to determine the S-wave velocity structures. The results have been compiled and published in a paper (Kudo et al., 2002). However, the deeper parts of the S-wave velocity structures have not been determined in their study due to relatively small array sizes. In September 2003, as a continuation of these array measurements, we conducted similar measurements at the two sites in the west part of Istanbul (Fig. 1). One is the Avcilar area (AVC) where heavy damage occurred during the 17 August 1999 earthquake and the other, near the airport where a permanent strong-motion site (DHM) is deployed by the Kandilli Observatory and Earthquake Research Institute of Bogazici University (KOERI).

On the other hand, the U.S. Geological Survey, in cooperation with KOERI, performed aftershock observations in western Istanbul to correlate site effects with the distribution of the damaged buildings. Ozel et al. (2002) and Cranswick
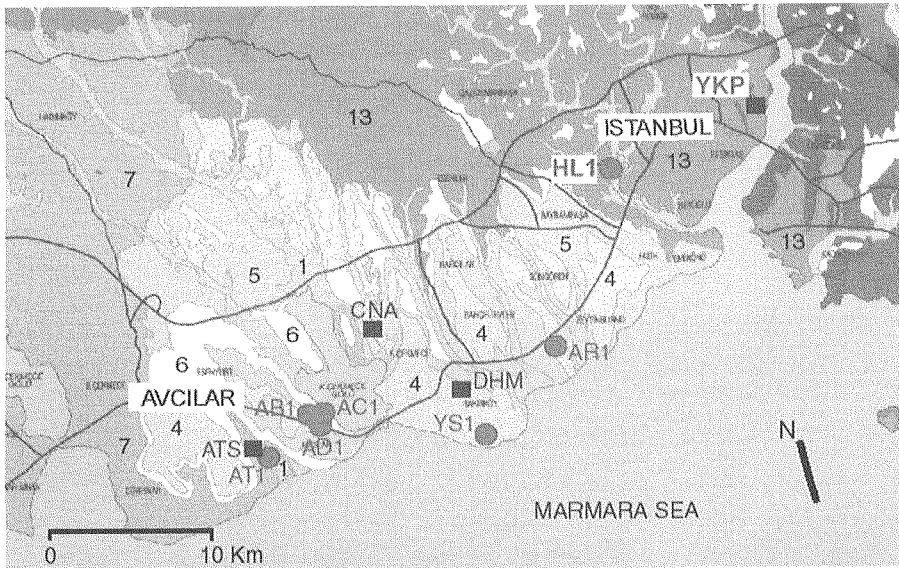
Fig. 1. Geotechnical bearing capacity map of Avcilar and west Istanbul (after Ozel
et al., 2002). The locations of temporary stations (a tripartite array AB1, AC1
and AD1, and HL1), and permanent strong motion sites (YKP and DHM) are
shown by circles and rectangles, respectively. The other stations are out of the
target of this study. The numbers on the map are; [1] Alluvium with low-
loading capacities where load capacity increases from 1 to 3; [4] alluvium with
good-loading capacity with weak zones locally; [5] alluvium with low-loading
capacity with increase probability of landslides on slopes reaching 14-15°; [6]
alluvium with high-loading capacity but landslides may occur where ground
water accumulates at bottom of slopes; [7] alluvium with low-loading capacities
with known damage to structures; [13] rock with high-loading capacities except
on slopes.

et al. (1999) studied the empirical amplification functions and the response of
buildings in the area. However, quantitative evaluation of the empirical
amplifications has not been done in these studies. It is important to evaluate
the empirical amplification functions based on the S-wave velocity structures.

The main aim of this study is to estimate the S-wave velocity structures at
two sites (AVC and DHM) especially for deeper parts, and to compare quantita-
tively the empirical amplification functions with the theoretical ones based on
the S-wave velocity structures. Firstly, we estimate phase velocities of
Rayleigh waves from vertical components of array records of microtremors.
The subsurface S-wave velocity structures are estimated by the inversion of the
Rayleigh-wave phase velocities. In the estimation, we combine the phase
velocity data from 1999 measurements and current measurements. Secondly,

we calculate amplification functions from the aftershock records of the 17 August 1999 earthquake and compare them with the theoretical ones based on the S-wave velocity structures estimated from microtremors.

2.   Estimation of S-wave Velocity Structures

2.1   Method

To extract surface waves from microtremor, two methods are available : the frequency-wavenumber method (f-k method) (Capon, 1969) and the spatial auto-correlation method (SPAC method) (Aki, 1957 ; Lacoss et al., 1969 ; Okada, 2003).   The both methods are based on the assumptions that microtremors are mainly composed of surface waves and are a spatiotemporally stationary stochastic process.   Phase velocities of Rayleigh waves are estimated from vertical components of microtremors, and then inverted to the subsurface S-wave velocity structure.   The f-k method can separate multimode surface waves as well as body waves but requires a number of seismometers more than that the SPAC method requires ; an array with fewer stations (say, less than 10) inevitably results in lower resolution.   Although the SPAC method cannot separate plural modes of dispersive surface waves as well as body waves, it requires an array of fewer stations.   An array for the SPAC method requires 4 stations as the minimum requirement and it is necessary to deploy stations in a circular configuration with one common station at the center
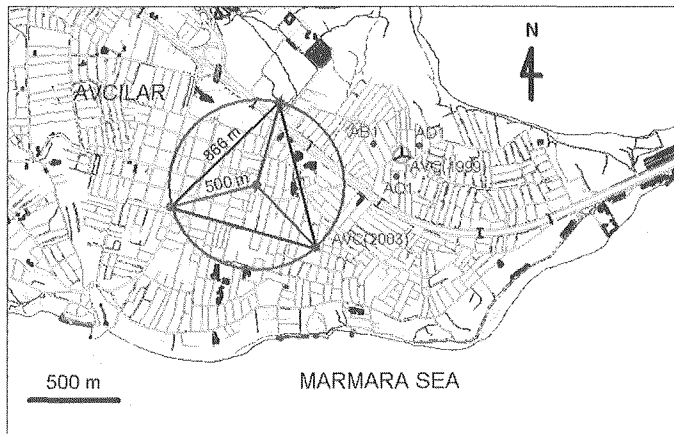

Fig. 2.   Map showing locations of array microtremor measurements at Avcilar area. The temporary tripartite array stations (AB1, AC1 and AD1) recording the aftershocks are also shown.

(see Fig. 2). The observable maximum wavelength may reach 10 times the radius of the array for the SPAC method (Miyakoshi et al., 1996). Further deliberations of the SPAC method can be found in the literature (e.g. Okada, 2003 ; Kudo et al. 2002). In this study, the SPAC method is applied to estimation of phase velocities.

The instruments used in this study were originally developed for a temporal observation of strong- and weak-ground motions (Kudo et al., 1998). It is composed of triaxial accelerometers with the highly damped (h~26) moving coil (the natural frequency of 3 Hz), a signal conditioner and a 24-bit data logger with Global Positioning System time synchronization. A flat response (-3 dB) of ground acceleration is attained from 0.1 Hz to an aliasing frequency. The sensor sensitivity is 1 V/g and optionally 5 V/g. The clipping level of a sensor is 150 cm/sec ; the maximum observable acceleration is 1 g at 1 Hz or 10 g at 10 Hz. The allowable input level of the data logger is selectable, 1 V or 5 V. The low-pass filter with cutoff frequencies at 2, 5 and 30 Hz is provided.

2.2 Estimation of Phase Velocities

We use only the vertical motion of microtremors to extract Rayleigh waves. Figures 2 and 3 show the array observation sites and details about the arrays are given in Table 1. Figure 4 shows an example of the velocity time histories integrated from the accelerations of microtremors that were simultaneously
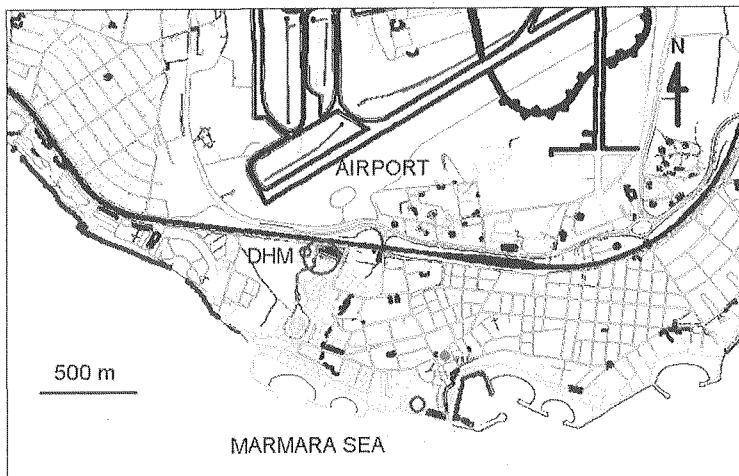

Fig. 3.   Map showing locations of array microtremor measurements at DHM site.

Table 1. Information about the array microtremor measurements. AVC*
denotes the array measurements performed in 1999. The array
size is a radius of the circular array. Phase velocities are
obtained in the frequency range shown below.

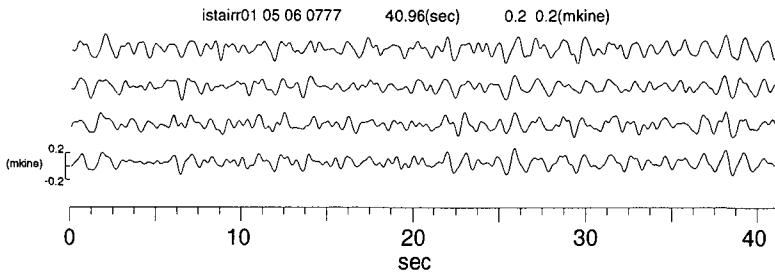| Site Name	Code	Coordinates	Arrays Size	Frequency Range
Avcilar	AVC	40.97N–28.72E	500 m	0.36~0.60 Hz
	AVC*	40.98N–28.73E	25 m–58 m–100 m	0.85~4.35 Hz
Airport	DHM	40.96N–28.81E	96 m–30 m	0.72~4.0 Hz

Fig. 4. An example of array microtremors (integrated ground velocity) at DHM site.
These traces are obtained through a low-pass filter with a cutoff frequency of 2
Hz. The array size (radius of the circular array) is 96 m.

recorded at DHM site, by a circular array with a radius of 96 m. The records
are obtained through a low-pass filter with a cutoff frequency of 2 Hz. It can
be easily seen that the waveforms are similar to each other.

   We divide the observed records of vertical component into time segments
with the length of 10.24 s or 20.48 s. We reject the time segments contaminated
by man-made noise (such as cars, trucks, man steps etc.). Then we evaluate the
rest of the time segments on the basis of coherency and power spectra. Figure
5 shows an example of power spectra for the time segments shown in Fig. 4.
Finally the time segments having good coherency and high power are selected.
The SPAC coefficients are calculated for various combinations of station
distances, as a function of frequency, and averaged for the selected time seg-
ments. The SPAC coefficients, finally averaged azimuthally, for a fixed dis-
tance between two stations at various frequencies, provide the phase velocity of
propagating waves in the array. Figure 6 shows one example of the average
SPAC coefficients for the AVC site, obtained from 25 time segments. For the
frequency range, obtained SPAC coefficients should be used up to a frequency
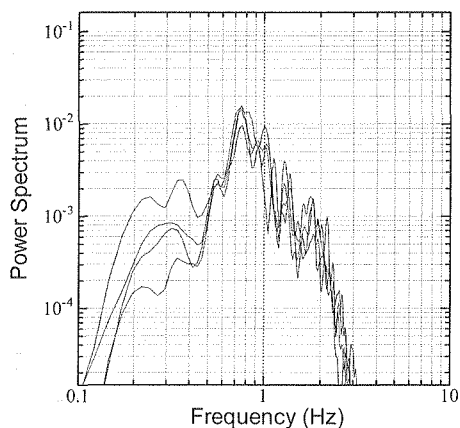around the first minimum (Okada, 2002). The vertical bars in Fig. 6 show the

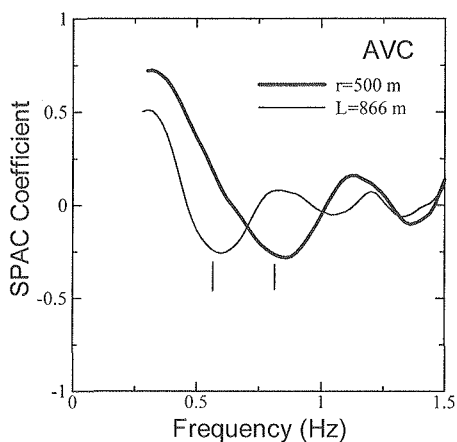Fig. 5. An example of the power spectra for the traces shown in Fig. 4.

Fig. 6. SPAC coefficients as a function of frequency for two distances at AVC site. r and L denote the array radius and the distance between the two corners of the triangle as shown in Fig. 2. The vertical bars show the frequencies around the first minimum of each curve. The SPAC coefficients up to these frequencies are available for the phase velocity estimation.

upper limit of the frequency range; the SPAC coefficients below this limit can be used in estimates of phase velocities. After obtaining phase velocities from different array radii, and overlapping them, we take the average of the phase velocities.

   In Fig. 7, we show observed phase velocities at AVC; the phase velocities in the frequency range of 0.85 to 4.35 Hz are taken from Kudo et al. (2002) who
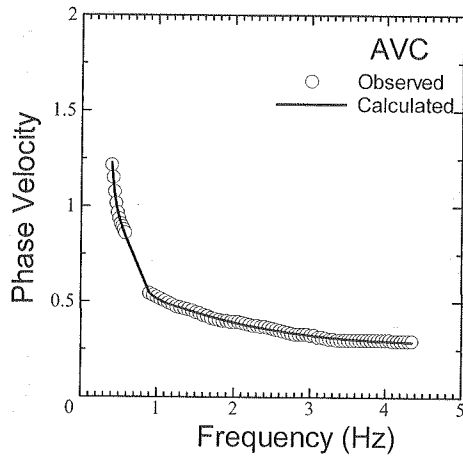
Fig. 7. Observed (circles) and calculated (solid line) phase velocities at AVC site.
The phase velocity data at the high frequency part (0.85 Hz~4.35 Hz) are taken
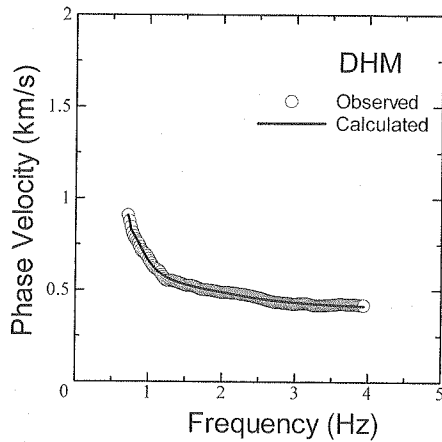from Kudo et al. (2002).

Fig. 8. Observed (circles) and calculated (solid line) phase velocities at DHM site.

performed array microtremor measurements in 1999. The current measure-
ments provide the higher phase velocities at low frequencies because of the
larger array size. The phase velocities at low frequencies are indispensable to
estimate a deep S-wave velocity structure. Figure 8 shows observed phase
velocities at DHM obtained by two arrays having radii of 30m and 96m (Table
1). These phase velocities have a similar trend as those at AVC ; however, the
velocity values are somewhat higher than those at AVC over the wide frequency

range.

2.3   S-Wave Velocity Structures

Next, we find a dispersion curve or an S-wave velocity structure that fits the observed phase velocities using the genetic algorithm (GA) (e.g., Yamanaka and Ishida, 1996).   In Figs. 7 and 8, we show the theoretical dispersion curves from the S-wave velocity structures shown in Fig. 9, estimated using the GA ; the theoretical curves fit the observed phase velocities well.   For the shallow structure at AVC, we employ the S-wave velocity structure obtained from the previous array microtremor measurements (Kudo et al., 2002).   For the DHM structure, the depth and velocity for the deepest layer may be ambiguous because of not enough phase velocity data at low frequencies (Fig. 8).

3.   Evaluation of Site Amplification Functions

3.1   Empirical Amplification Functions

As a post-earthquake campaign, the US Geological Survey (USGS) in co-operation with the KOERI deployed portable digital seismographs at seven free-field sites in western Istanbul to observe aftershocks during the period from 24 August to 2 September in 1999.   These included a small aperture ($\sim$200 m) tripartite array in a heavily damaged neighborhood of Avcilar (AB1, AC1 and AD1 ; see Fig. 2).   In the near surface, the Avcilar area is underlain by as much
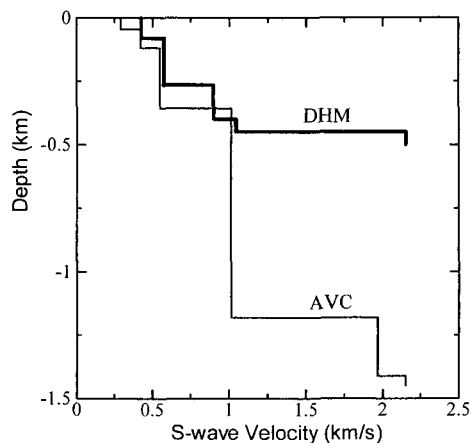

Fig. 9.   Estimated S-wave velocity structures at AVC and DHM sites, corresponding to the phase velocities given in Figs. 7 and 8.

Table 2. Information about aftershocks used in calculation of empirical amplification functions.

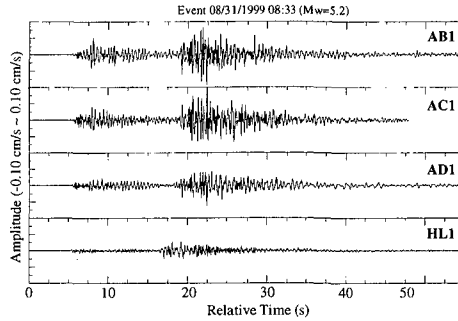| Event No	Date	Time	Coordinates	Magnitude
1	31. 08. 1999	8 : 10 : 51	40.75N–29.92E	5.2
2	31. 08. 1999	8 : 33 : 00	40.78N–29.96E	4.6
3	31. 08. 1999	22 : 28 : 21	40.63N–29.09E	4.1

Fig. 10. Ground velocity records (NS-components) at the tripartite stations (AB1, AC1 and AD1) and the reference station (HL1). The tripartite stations are deployed at a triangle 200 m apart as shown in Fig. 2.

as 200 m of poorly lithified Quaternary Pliocene and Miocene sands and gravel, marls, and limestone (Brinkman, 1976). One station was deployed at a hard-rock site (HL1 in Fig. 1) composed of low-grade metamorphosed or at least indurated Devonian sandstones and siltstones (Cranswick et al., 1999). This station has been taken as a reference station for the classical spectral ratio calculations to estimate the empirical amplification functions for the tripartite array stations. Furthermore, we use YKP site as a reference station for the calculation of empirical amplification function at the permanent strong motion site, DHM.

We select three moderate-size earthquakes with the magnitudes of 4.1, 4.6 and 5.2 (Table 2) to calculate the empirical amplification functions for the tripartite array stations of AB1, AC1 and AD1. These events are selected since they have a good signal-to-noise ratio. We use only NS components of the records ; this component represents mainly the transverse component since the epicenters of all three earthquakes are located in the just east direction of the array stations. As an example, the NS components at the tripartite array stations and reference station are shown in Fig. 10. The PGV values at the
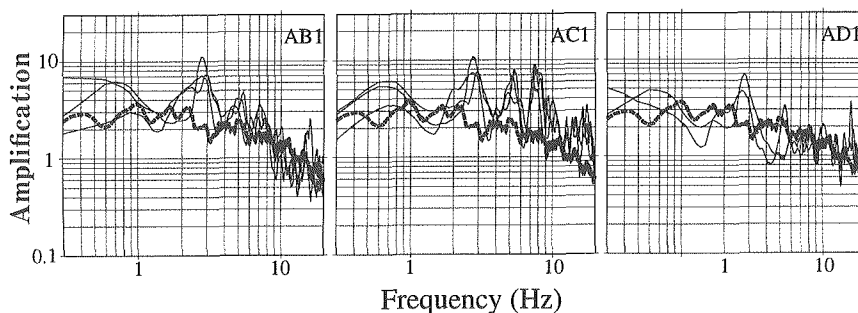
Fig. 11. Theoretical (bold lines) and empirical (thin lines) amplification functions at the tripartite array stations (AB1, AC1 and AD1). The empirical amplification functions calculated from each event given in Table 2 are plotted separately.
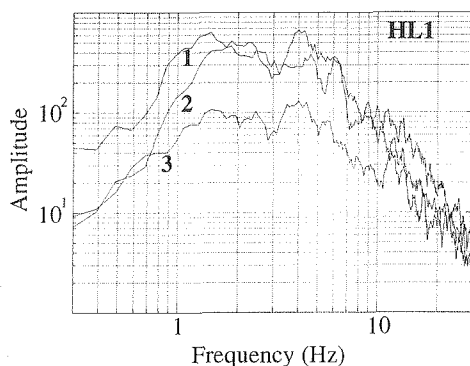

Fig. 12. Fourier amplitude spectra for the aftershocks (Table 2) recorded at the reference site HL1. The spectra show that there is a noticeable trough at 3 Hz for all the three events. Since this station is used as denominator in calculation of empirical amplification functions, the differences between the empirical and theoretical amplification functions at 3 Hz shown in Figure 11 can be attributed to the trough. The numbers show the event numbers in Table 2.

array stations are three to four times larger than that at HL1. We calculate the amplification functions by taking the S-wave spectral ratio of the tripartite array stations to the reference site HL1. In Fig. 11, we show the amplification functions for three events at these stations. All the three spectral ratios at AB1, AC1 and AD1 show a remarkable peak at about 3 Hz, which reaches to a factor of about 10. On the other hand, Figure 12 depicts the S-wave spectra at HL1 from the selected three events, which show a trough at about 3 Hz. The spectral trough may be due to a topographic effect since the surrounding area of site HL1 is a hillside. Therefore, we cannot attribute the common peak at

about 3 Hz in the amplification functions to a site effect at the tripartite array
stations.

Ozel et al., (2002) calculated the empirical amplification functions at DHM
by the classical spectral ratio method for several aftershocks (Table 1 in Ozel et
al. 2002) ; YKP located on a hard-rock site was used as the reference station
(see Fig. 1).   Figure 13 shows the average amplification function (bold line) for
this station, taken from Ozel et al. (2002).   This station shows amplification
levels of 3-5 at frequencies from about 0.5 to 2.0 Hz.

3.2   Theoretical Amplification Functions

Using the S-wave velocity structures determined in this study, we calculate
theoretical site amplification functions for the observation sites of AVC and
DHM by the one-dimensional propagator-matrix method (Aki and Richards,
1980) for a vertically incident S wave.   We assume that the quality factor Q is
frequency independent and constant for each layer because of no available
information (Table 3).   In order to calculate the amplification function, we take
the ratios of the site response at AVC to that at HL1, in the same way, DHM
to YKP.   Here, we use the preliminary S-wave velocity structure estimated by
Kudo et al. (in preparation) for the reference sites of YKP and HL1 (see Table
3).   Then we compare these theoretical amplification functions with the empiri-
cal amplification functions mentioned above.   The results are plotted on the
empirical ones in Figs. 11 and 13.

Table 3.   S-wave velocity structures obtained at AVC and DHM sites.   The
shallow part at AVC site separated by thin line is taken from Kudo
et al., (2002).   Also given are the velocity structures at YKP and
HL1 sites used in calculations of 1D-theoretical amplification func-
tion.   The layer with an S-wave velocity of 2.15 km/s is assumed as
bedrock in the calculations.

AVC			DHM			YKP and HL1		
Vs (km/s)	H (m)	Q	Vs (km/s)	H (m)	Q	Vs (km/s)	H (m)	Q
0.291	46	30	0.424	80	30	0.20	1	30
0.434	91	30	0.575	185	30	2.15	～	200
0.584	239	100	0.897	134	100			
1.012	824	150	1.043	50	100			
1.967	231	200	2.15	～	200			
2.15	～	200						

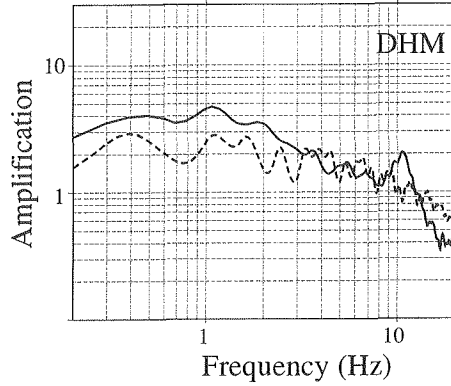H : layer thickness, Q : assummed quality factor.

Fig. 13.   Theoretical (dashed line) and empirical (bold line) amplification functions at DHM site.   The empirical amplification function is taken from Ozel et al. (2002).

As shown in Fig. 11, there is generally a good agreement between the empirical and theoretical amplification functions for AVC site, while the observed one at AC1 shows higher amplifications at high frequencies (>3 Hz).   The fairly good agreement between the empirical and theoretical amplifications at sites AB1 and AD1, except at the peak around 3 Hz, indicates that the S-wave velocity structure estimated by the array microtremor measurements can be considered as the representative one for AVC site.   However, apparent differences at high frequencies for AC1 site point out that the shallow velocity structure beneath AC1 differs from those beneath AB1 and AD1 in spite of about 200 m apart from each other.

For the strong motion site DHM, in Fig. 13, fundamental predominant frequencies of the empirical amplification function can be explained well by the theoretical one.   However, the empirical amplification function is slightly greater (less than a factor of 2) than that of theoretical one for low frequencies (<2 Hz).   The main reason may be due to the frequency range of the phase velocities (Table 1) determined by the SPAC method.   The lower frequency limit of the phase-velocity data is 0.7 Hz and hence the inverted S-wave velocity structure may not represent the real structure for deeper parts as mentioned before.

4. Conclusion

We conducted array measurements of microtremors at two sites, AVC and DHM, in the west part of Istanbul, as a continuation of the same type observa-

tions carried out just after the 17 August 1999 Izmit earthquake, to estimate the S-wave velocity structures beneath these sites. We used the SPAC method in estimation of phase velocities of Rayleigh waves, and the genetic algorithm in estimation of the S-wave velocity structures down to a depth of about 1 km. Then the empirical amplification functions derived from aftershock records were compared with the theoretical ones calculated based on the S-wave velocity structures estimated in this study. We obtained reasonably a good agreement between them, except one site of the tripartite array stations in AVC. The S-wave velocity structures estimated in this study provide basic data for prediction of strong-ground motion in Istanbul.

Acknowledgments

References

Aki, K., 1957. Space and time spectra of stationary stochastic waves, with special reference to microtremors. Bull. Earthq. Res. Inst., **35**, 415-456.

Aki, K. and Richards, P. G., 1980. Quantitative Seismology, Vol. 1, W.H. Freeman and Company Press, San Francisco, pp. 557.

Brinkman, R., 1976. Geology of Turkey, Ferdinant Enke Verlug, Stuttgart, Germany, pp. 158.

Capon, J., 1969. High-resolution frequency-wavenumber spectrum analysis, Proc. IEEE, **57**, 1408-1418.

Cranswick, E., O. Ozel, M. Meremonte, M. Erdik, E. Safak, C. Muller, D. Overturf, A. Frankel, 1999. Earthquake damage, site response, and building response in Avcilar, west of Istanbul, Turkey. International Journal for Housing Science and its Applications, ISSN 0146-6518, Special Issue: Kocaeli Earthquake 1999, Oktay Ural, Editor-In-Chief, Vol. 24, No. 1, 85-96.

Kudo, K., M. Takahashi, M. Sakaue, T. Kanno, H. Kakuma and D. Tsuboi, (1998). A highly over-damped moving coil type accelerometer for mobile strong-motion observation and its performance tests. Report of Grant-in-Aid for Scientific Research-07558056 (in Japanese with English abstract).

Kudo, K., T. Kanno, H. Okada, O. Ozel, M. Erdik, T. Sasatani, S. Higashi, M. Takahashi and K. Yoshida, 2002. Site-specific issues for strong-ground motions during the Kocaeli, Turkey earthquake of 17 August 1999, as inferred from array observations of microtremors and aftershocks. Bull. Seism. Soc. Am. **92**, 1, 448-465.

Lacoss, R.T., E.J. Kelly, and M.N. Toksoz, (1969). Estimation of seismic noise structure using array, Geophysics **34**, 21-38.

Miyakoshi, K., H. Okada and S. Ling, 1996.   Maximum wavelength possible to estimate phase velocities of surface waves in microtremors. Proceedings of the 94th SEGJ Conf., Society of Exploration Geophysicist, Japan, 178-182 (in Japanese).

Okada, H., 2002.   Remarks on the efficient numbers of observation points for the spatial auto-correlation method applied to array observation of microtremors.   Assessment of Seismic Local-Site Effects at Plural Test Sites (Project Coordinator : Kudo, K.), The Ministry of Education, Science, Sports and Culture, Research Grant No : 11694134, pp : 1-13.

Okada, H., 2003.   The microtremor survey method, Geophysical Monograph Series, **12**, Society of Exploration Geophysicists, pp. 135.

Ozel, O., E. Cranswick, M. Meremonte, M. Erdik and E. Safak, 2002.   Site effects in Avcilar, west of Istanbul, Turkey, from strong- and weak motion data.   Bull. Seism. Soc. Am., **92**, 1, 499-508.

Yamanaka, H. and H. Ishida, 1996.   Application of genetic algorithms to an inversion of surface-wave dispersion data.   Bull. Seism. Soc. Am. **86**, 436-444.